

High-efficiency large-angle reflective composite polarization grating

Zhi-Wei Zhao, Cheng-Miao Wang, Song-Zhen Li, Wan Chen, Yong-Gang Liu, Quan-Quan Mu, Zeng-Hui Peng, Qi-Dong Wang, Li Xuan & Ru-dong Wei


To cite this article: Zhi-Wei Zhao, Cheng-Miao Wang, Song-Zhen Li, Wan Chen, Yong-Gang Liu, Quan-Quan Mu, Zeng-Hui Peng, Qi-Dong Wang, Li Xuan & Ru-dong Wei (2019): High-efficiency large-angle reflective composite polarization grating, *Liquid Crystals*, DOI: [10.1080/02678292.2019.1633584](https://doi.org/10.1080/02678292.2019.1633584)

To link to this article: <https://doi.org/10.1080/02678292.2019.1633584>



Published online: 15 Jul 2019.



Submit your article to this journal 



View Crossmark data 



High-efficiency large-angle reflective composite polarization grating

Zhi-Wei Zhao^{a,b}, Cheng-Miao Wang^{a,b}, Song-Zhen Li^{a,b}, Wan Chen^{a,b}, Yong-Gang Liu^a, Quan-Quan Mu^{a,b}, Zeng-Hui Peng^{a,b}, Qi-Dong Wang^a, Li Xuan^{a,b} and Ru-dong Wei^{a,b}

^aState Key Laboratory of Applied Optics, Changchun Institute of Optics, Fine Mechanics and Physics, Chinese Academy of Sciences, Changchun, Jilin, China; ^bCenter of Materials Science and Optoelectronics Engineering, University of Chinese Academy of Sciences, Beijing, Jilin, China

ABSTRACT

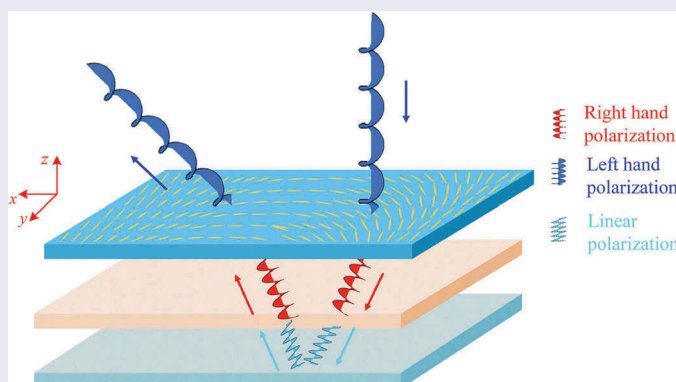
We introduce and demonstrate a new structure of polarisation grating which can substantially enlarge the deflection angle. We derive the polarisation state of a beam passing through the reflective composite polarisation grating by Jones matrix and build a rigorous simulation about the deflection angle of reflective composite polarisation grating using finite-element analysis. The theoretical diffraction efficiency of the reflective composite polarisation grating can reach up to 90%. The experimental result of deflection angle of the reflective composite polarisation grating is consistent with that of simulation. The reflective composite polarisation grating could be expected to be applied in augmented reality system, spectroscopy, optical telecommunications, non-mechanical beam steering and so on.

ARTICLE HISTORY

Received 16 April 2019
Accepted 15 June 2019

KEYWORDS

Liquid crystal; polarisation grating; reflective mode; beam steering



1. Introduction

Liquid crystal device (LCD) is widely in optical devices such as information display [1], spatial light modulator [2], beam shaping, beam steering and diffracted gratings for properties of optical anisotropy and electrically tunability [3–6]. Polarisation grating (PG) are diffractive elements based on a spatial periodical variation of molecular orientation, resulting in a local modulation of birefringence. PG exhibits several unique properties because of periodical orientation, such as high efficiency in one diffraction order, converting the polarisation state of the input light. They can transform linear polarisation light into left or right circularly polarised light. The deflection angle of PG is inversely proportional to the grating period, both the deflection angle and period accord the

grating equations in $\theta_{diff} = \lambda/\Lambda$ under the condition of normal incidence. To get a larger deflection angle, we need PG with a smaller period. However, for PG, there is no report yet which experimentally demonstrates efficiency approaching 100% when the grating period is near or below the wavelength, especially for visible waves [7]. The full numerical analysis of PG reported by Michael J. Escuti reveals the relationship between the diffraction efficiency and the grating period especially when the grating parameters Λ/λ are small [8,9], and a high linear birefringence material is needed to achieve a high diffraction efficiency and a larger deflection angle. To achieve the large diffraction angle, Gao Kun reported a Pancharatnam phase deflector based on dual-twist design with 90% diffraction efficiency and 40° deflection

angle [10–12]. Xiao Xiang and Michael J. Escuti reported LCpolymer Bragg polarisation grating with 335 nm grating period and more than 85% efficiency, and the LCpolymer Bragg polarisation grating could achieve a 51° deflection angle and an optimised angular wavelength [13,14]. Wu Shin-Tson reported a reflective polarisation volume grating with a 50° deflection angle and over 90% efficiency [15]. Tremendous researches have been implemented in order to optimise response time [16–18], angular wavelength [19–21] and others. What can be expected is that the PG with large deflection angle and high diffraction efficiency could be a promising element in laser beam steering [22–24], augment reality system [25,26] and so on.

In this article, we design a novel structure of polarisation grating which can be fabricated simply and easily enlarge the deflection angle of polarisation grating. We implement a simulation about the deflection angle of the novel structural polarisation grating. The experimental result of the deflection angle is consistent with the simulation result. Theoretically, the novel structure of polarisation grating could achieve 90% diffraction efficiency, and the experimental diffraction efficiency is lower than that of simulation. The more specific experimental results are discussed in Results and Discussion.

2. Theoretical basis

For the LCPolarisation grating (LCPG), there are two ways that LC molecules can be distributed in a grating period, as shown in Figure 1.

For PG in Figure 1(a), the relationship between input light and output light at on position in the aperture of a primary Pancharatnam phase device can be expressed as

$$[E_{out}] = [M(\Gamma, \theta)][E_{in}]$$

Here

$$[M(\Gamma, \theta)] = [R(-\theta)] \begin{bmatrix} e^{-i\Gamma/2} & 0 \\ 0 & e^{i\Gamma/2} \end{bmatrix} [R(\theta)]$$

$\Gamma = 2\pi\Delta n d/\lambda$, θ is the angle between the slow axis and x axis, $\theta = \pi x/\Lambda$ and $[R(-\theta)]$ is a rotation matrix, We can write this as

$$[M(\Gamma, \theta)] = \begin{bmatrix} \cos \theta & -\sin \theta \\ \sin \theta & \cos \theta \end{bmatrix} \begin{bmatrix} e^{-i\Gamma/2} & 0 \\ 0 & e^{i\Gamma/2} \end{bmatrix} \begin{bmatrix} \cos \theta & \sin \theta \\ -\sin \theta & \cos \theta \end{bmatrix}$$

Inserting

$$e^{i\Gamma/2} = \cos \Gamma/2 + i \sin \Gamma/2, e^{-i\Gamma/2} = \cos \Gamma/2 - i \sin \Gamma/2$$

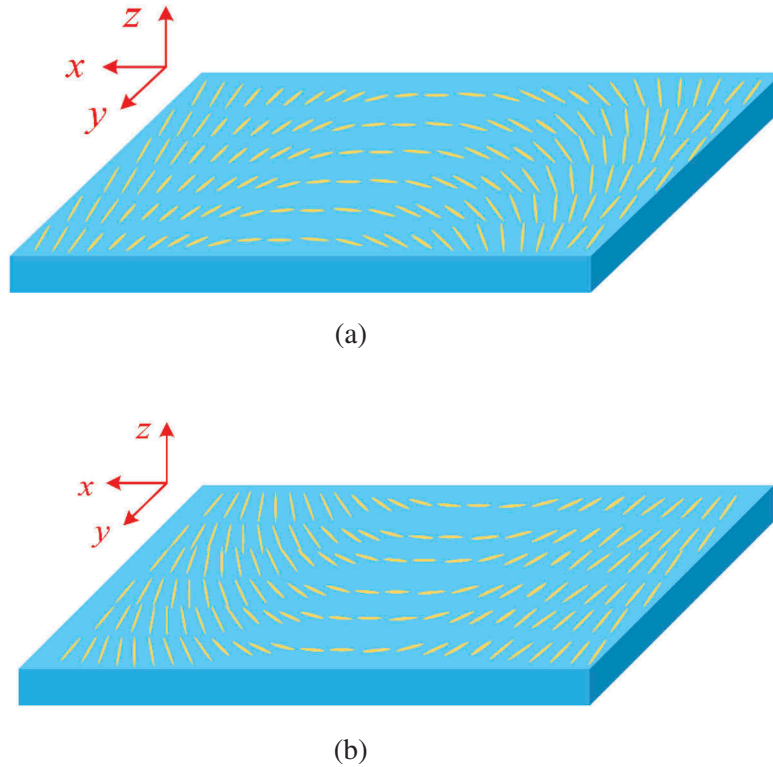


Figure 1. (Colour online) (a) Liquid crystal molecules of PG distributed counterclockwise; (b) liquid crystal molecules of PG distributed clockwise.

$$\begin{aligned}
[M(\Gamma, \theta)] &= \cos \frac{\Gamma}{2} \begin{bmatrix} 1 & 0 \\ 0 & 1 \end{bmatrix} + i \sin \frac{\Gamma}{2} \begin{bmatrix} -\cos 2\theta & \sin 2\theta \\ \sin 2\theta & \cos 2\theta \end{bmatrix} \\
&= \cos \frac{\Gamma}{2} \begin{bmatrix} 1 & 0 \\ 0 & 1 \end{bmatrix} + \frac{i}{2} \sin \frac{\Gamma}{2} \begin{bmatrix} -(e^{i2\theta} + e^{-i2\theta}) & -i(e^{i2\theta} - e^{-i2\theta}) \\ -i(e^{i2\theta} - e^{-i2\theta}) & (e^{i2\theta} + e^{-i2\theta}) \end{bmatrix} \\
&= \cos \frac{\Gamma}{2} \begin{bmatrix} 1 & 0 \\ 0 & 1 \end{bmatrix} + \frac{i}{2} \sin \frac{\Gamma}{2} e^{i2\theta} \begin{bmatrix} -1 & -i \\ -i & 1 \end{bmatrix} + \frac{i}{2} \sin \frac{\Gamma}{2} e^{-i2\theta} \begin{bmatrix} -1 & i \\ i & 1 \end{bmatrix}
\end{aligned}$$

The relationship between input light and output light considering circularly polarised input light is

$$\begin{bmatrix} E_{x-out} \\ E_{y-out} \end{bmatrix} = \begin{bmatrix} 1 \\ \pm i \end{bmatrix}$$

This results in

$$\begin{bmatrix} E_{x-out} \\ E_{z-out} \end{bmatrix} = \cos \frac{\Gamma}{2} \begin{bmatrix} 1 \\ \pm i \end{bmatrix} - i \sin \frac{\Gamma}{2} e^{-i(\pm 2\theta)} \begin{bmatrix} 1 \\ \mp i \end{bmatrix}$$

The above equation makes it clear that the polarisation of input light is revised. Input light achieves a phase shift determined by the angle θ , which is the angle the director is rotated about a normal to the plane of the layer.

For PG in Figure 1(b), the Jones matrix of output light is

$$\begin{bmatrix} E_{x-out} \\ E_{z-out} \end{bmatrix} = \cos \frac{\Gamma}{2} \begin{bmatrix} 1 \\ \pm i \end{bmatrix} - i \sin \frac{\Gamma}{2} e^{-i(\mp 2\theta)} \begin{bmatrix} 1 \\ \mp i \end{bmatrix}$$

The main difference between two the Jones matrix of the output light is the sign of the angle 2θ which determines the deflection direction of output light. The input light is the right circular polarised, after passing through the PG in Figure 1(a and b), the output diffraction light is the same polarisation with opposite deflection direction. If the input light is incident along the positive z axis and negative z axis to PG, PG along positive z axis is Figure 1(a). and negative

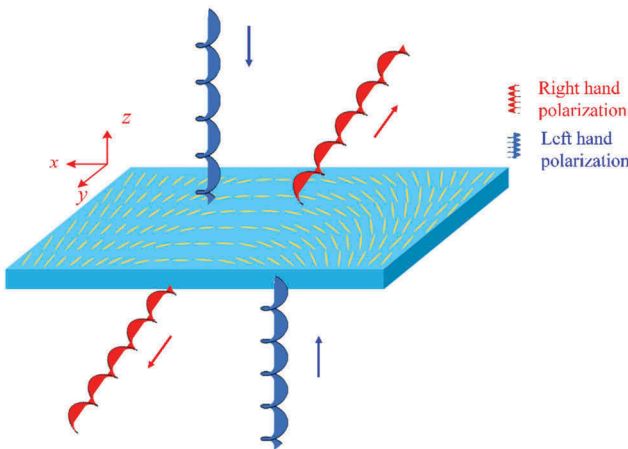


Figure 2. (Colour online) The schematic of optical performance observed in the experiment when input light is along the positive z -axis and negative z -axis.

z axis is Figure 1(b). Figure 2 shows the direction of deflection light when input light is incident along the positive z axis and negative z axis.

R. K. Komanduri and M. J. Escuti experimentally demonstrated a reflective LCpolarisation grating (RPG) [27]. One regular indium tin oxide substrate and a reflective substrate is to create a cell, then exposed to an interference pattern formed between two orthogonally circularly polarised UV laser beam. To avoid the degradation of the recording hologram by the reflection entirely, they employ a thin layer to absorb the recording wavelength, arranged between the reflective substrate and the photo-alignment material. Since the reflective-mode LCPG is optimally formed with half the cell thickness of the transmission mode (i.e. a quarter-wave retardation), the minimum possible grating period Λ can be reduced to half. Figure 3 shows the schematic of optical performance observed in the experiment when the input light is along the reflective LCPG which meets the half-wave retardation rather than the quarter-wave retardation.

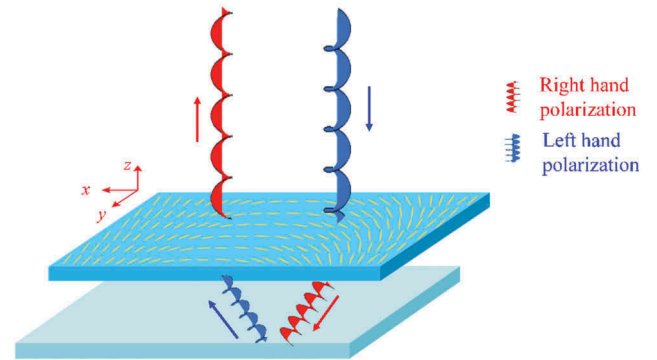


Figure 3. (Colour online) The schematic of optical performance when input light is along the negative z -axis into reflective liquid crystal polarisation.

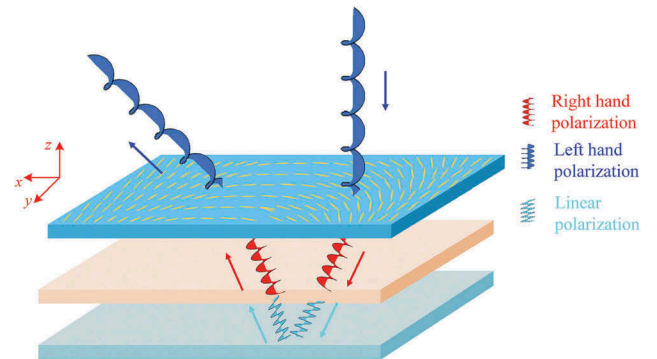


Figure 4. (Colour online) The schematic of optical performance when input light is along negative z -axis into reflective composite liquid crystal polarisation grating.

We can observe that the final deflection beam passing through the reflective LCPG remains in the same direction as the incident beam but with the opposite polarisation which is same as the PG. The polarisation of input light is reversed twice by PG with half-wave retardation and the mirror, The beam remains the same polarised state as the incident beam before secondly hitting into the PG. That is why the final deflection beam remains the same direction other than diffracts secondly.

3. Structure design

The final deflection beam should diffract twice theoretically when we can change the polarisation of the light the same as the incident light before secondly hitting into the PG. In fact, it can be achieved by combination of a quarter-wave plate and a mirror, as shown in Figure 4.

The fast axis of the quarter-wave plate is along x -axis, and the Jones matrix of light passing through the quarter wave plate-mirror-quarter wave plate is

$$M_Q = \begin{bmatrix} 1 & 0 \\ 0 & i \end{bmatrix} \begin{bmatrix} -1 & 0 \\ 0 & 1 \end{bmatrix} \begin{bmatrix} 1 & 0 \\ 0 & i \end{bmatrix} = \begin{bmatrix} -1 & 0 \\ 0 & -1 \end{bmatrix}$$

$$\begin{bmatrix} E_{Qx-out} \\ E_{Qz-out} \end{bmatrix} = M_Q \begin{bmatrix} E_{Qx-in} \\ E_{Qz-in} \end{bmatrix}$$

$$\begin{bmatrix} E_{Qx-in} \\ E_{Qz-in} \end{bmatrix} = \begin{bmatrix} 1 \\ \pm i \end{bmatrix}$$

$$\begin{bmatrix} E_{Qx-out} \\ E_{Qz-out} \end{bmatrix} = - \begin{bmatrix} 1 \\ \pm i \end{bmatrix}$$

From the above equations, we can derive that light remains their polarisation state when it passes through the quarter-wave plate-mirror-quarter wave plate. The light can diffract twice when passing through the reflective composite polarisation grating (RCPG). The deflection angle of the RCPG is twice as much as PG with the same grating period. However, the diffraction efficiency of the RCPG would decrease compared with that of PG because of its unique structural property. There are two factors that affect the diffraction efficiency: light beam is oblique incidence when it passes through the PG twice, the effective phase retardation varies with incident angle, the phase retardation of the PG meets the half-wave retardation at normal incidence direction; another factor is that there are too many Fresnel reflections and absorption scattering when the light beam passes through the RCPG including polarisation grating LC layer, photo-alignment layer, glass substrate, indium tin oxide (ITO)

thin film, rubbed-oriented layer, wave-plate LC layer and the mirror.

4. Experiments

The method of the fabrication process of the RCPG in this article is similar to that used by Oh and Escuti. It involves writing a polarisation holography into photo-alignment materials [28,29]. Polarisation holography records the polarisation distribution of the interference of two beams, rather than the intensity fringes. Two coherent beams with orthogonal circular polarisation are superimposed with an angle deciding the polarisation grating period, which creates a spatially varying linear polarisation distribution. Photo-alignment material makes LC molecules align following the linear polarisation distribution. The fabrication set-up is described schematically in [18]. The 325-nm laser is coupled into the hole by the micro-objective, and then collimated by a lens. The collimated beams are divided into beams with the same intensity by the BS. The two beams are reflected by mirrors and pass through the quarter-wave plate which fast axis are perpendicular to each other, respectively, and superimposed on the sample creating a spatially varying linear polarisation distribution.

The RCPG is composed of polarisation grating, quarter-wave plate and mirror. We can achieve the RCPG with only two indium-tin-oxide substrates avoiding Fresnel interface reflection. A passive polarisation grating is fabricated with one indium-tin-oxide substrate. The substrate surface without ITO thin film is spin coated with photo-alignment at 1000 rpm for 10 s and 3000 rpm for 40 s, then dried at 150°C for 30 min. For the photo-alignment layer, we use the photo-sensitive polymer called linear photo-polymerisable polymer (LPP, rolic-103) layer. The substrate is exposed with orthogonal circular polarisation beams from He-Cd (325 nm) laser, and the dose of exposure is 5 J/cm². After exposing, a reactive mesogen film is spin coated on the LPP layer, and the reactive mesogen molecules self-align to the LPP molecules. The optical retardation of the reactive mesogen film must equal to the half of the wavelength of interest; however, it is impossible to deposit a single reactive mesogen layer thick enough to provide the required retardation, because the monomers tend to orient themselves out of the plane of the film to reduce the high elastic energy. To overcome this, we need to coat multiple thin reactive mesogen layers. Each layer self-aligns to the one beneath it and is then polymerised to lock in the desired orientation.

In this article, we use ROF dissolved in solvent propylene-glycol-methyl-ether-acetate (PGMEA) with

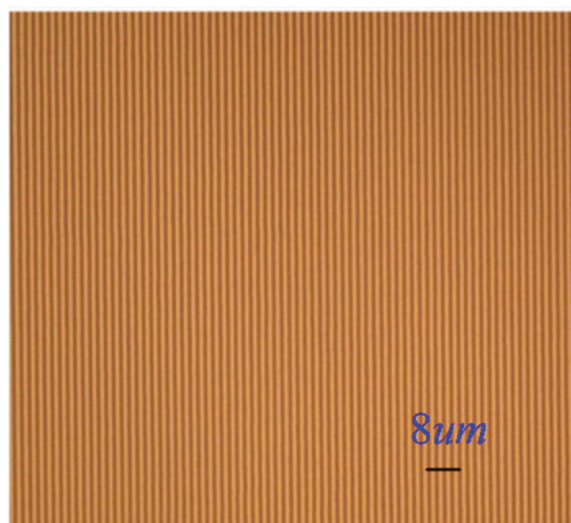


Figure 5. (Colour online) The micrograph of polarisation grating under a polarised optical microscope, grating period is 4 μm , the scale bar is 8 μm .

a concentration of 50% by weight. The reactive mesogen-PEMGA solution is spin coated at the LPP layer at 500 rpm for 10 s and 2000 rpm for 40 s after the holographic exposure. During subsequent exposure to UV lamps for 2 min in an N_2 -rich environment, the LC monomers form a cross-linked polymer. The process continues until the polarisation gratings meet the half-wave retardation. In this article, we spin three-layer ROF-PGMEA solution to achieve the half-wave retardation (532 nm). Another substrate is aluminium mirror. Polyimide is spin coated at aluminium mirrors and another substrate surface with ITO thin film at 1000 rpm for 10 s and 6000 rpm for 40 s, then dried at 150°C for 10 min and 235°C for 30 min. The polyimide film gets parallel orientation by rubbed. Two substrate surface with ITO thin film opposite are assembled together separated by 4- μm spacers. The cell was filled by capillary action with the LC mixture Mo16 (from DIC) above the clearing temperature (120) and slowly cooled down into the nematic phase.

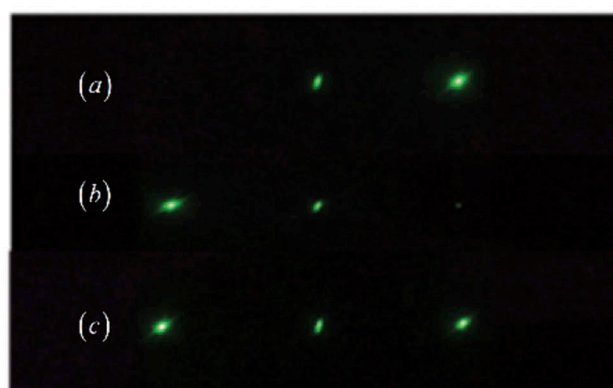


Figure 7. (Colour online) The far-field diffraction of polarisation grating. (a) Diffraction pattern of left circular polarisation incident light. (b) Diffraction pattern of right circular polarisation incident light. (c) Diffraction pattern of linear polarisation incident light.

5. Results and discussion

Figure 5 shows the micrographs of the PG observed under a polarised optical microscope. The space-variant directors of LC are exhibited by the continuous change of the brightness under the polarised optical microscope. For the regions that the LC directors are around 45° with respect to the polariser or analyser, we can see the bright domains, and for the regions that the LC directors are nearly parallel to the polariser or analyser, we can see the dark domains. Therefore, the bright-to-dark domains alternate twice along with the LC directors turning through π under the polarised optical microscope. When rotating the analyser, the bright and dark domains interconvert gradually, confirming the continuous varying of the director.

A laser ($\lambda = 532\text{nm}$) was used as probe beam to investigate the diffraction properties of the RCPG, as presented in Figure 6. The laser passed through the polariser, quarter-wave plate and the sample successively, and then was detected by the detector.

Figure 7 shows the diffraction patterns of the PG with different polarisation incident light. Only the 1st order and

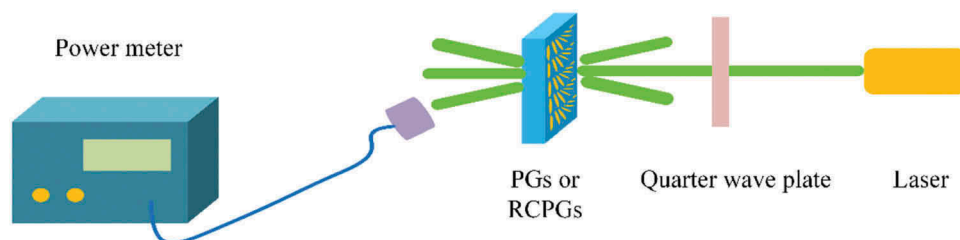


Figure 6. (Colour online) The schematic experimental setup for measuring the diffraction characteristics of a PG or an RCPG with a laser.

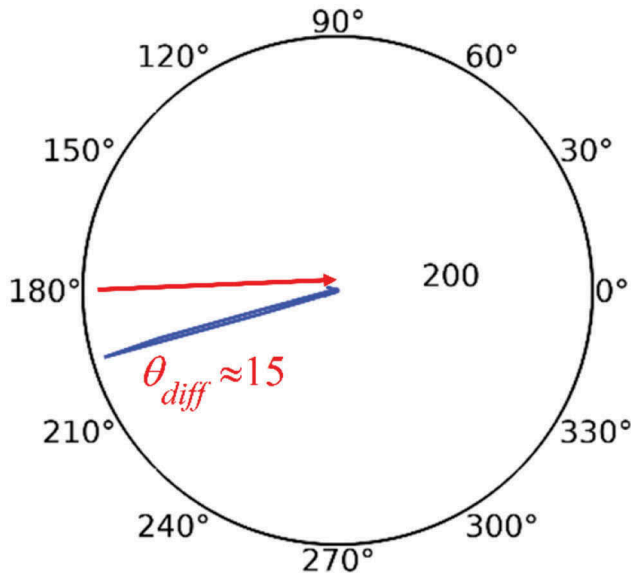


Figure 8. (Colour online) The simulation result of RCPG diffraction angle for left-handed circularly polarised incident light, the grating period is 4 μm .

the 0th order can be observed, indicating that the phase retardation matches the half-wave condition, and if the incident light is left circular polarisation, the diffraction light is almost at the -1st order as shown in Figure 7(a), for the right circular polarisation incident light, the diffraction light is almost at the $+1\text{st}$ order as shown in Figure 7(b), for the linear polarisation incident light, the diffraction light is almost at both the $+1\text{st}$ order and -1st order as shown in Figure 7(b). For the circular polarisation incident light, the 1st-order diffraction efficiencies are both up to the 98%, the power of both the zero-order diffraction light and the first-order diffraction light is 84 uw .

We built a rigorous model using finite-element analysis. We assume the polarisation grating thickness and

LC birefringence Δn satisfy the half-wave phase retardation condition. A quarter-wave phase retardation is 532 nm. The reflector is aluminium film. The stimulated RCPG diffraction angle is as shown in Figure 8(a). The grating period is 4 μm . We can get that the diffraction angle of RCPG $\theta = 15.2^\circ$ is two times as big as the polarisation grating which works in transmission mode. We also stimulate that the diffraction efficiency of PG varies with the incident angle, as shown in Figure 9.

We can get the diffraction efficiency of PG is related to the incident angle from Figure 9. The diffraction efficiency would decrease if the input light beam is off the normal incidence. For RCPG, the beam is oblique incidence on polarisation grating when it is reflected by the mirror, the oblique incidence angle is equal to the deflection angle of polarisation grating which is unavoidable, as shown in Figure 4. Thus, the diffraction efficiency of the RCPG is lower than transmission mode PG, and Fresnel reflection loss caused by multiple interfaces of RCPG further affects the output beam energy and diffraction efficiency. The diffraction efficiency decreases about 3%, but also reaches up to 90%.

Figure 10(a) shows the diffraction patterns of the RCPG with different polarisation incident light. We can observe 6 light spot lined in two rows because the incident light, spot F in Figure 10(a) is coming obliquely into the RCPG in order to measure the diffraction efficiency of all the diffraction orders, as shown in Figure 10(b). Spot C in Figure 10(a) is spot C1 and C2 in Figure 10(b) that spot C1 and spot C2 is overlapped. Spot C and spot F would be overlapped if the incident light is coming normally into the RCPG. For Figure 10(a) incident light is left-handed circularly polarised light, the diffraction angle between spot A and spot C is about 15 degrees which is in line with simulation in Figure 8, the power of light spot A depends

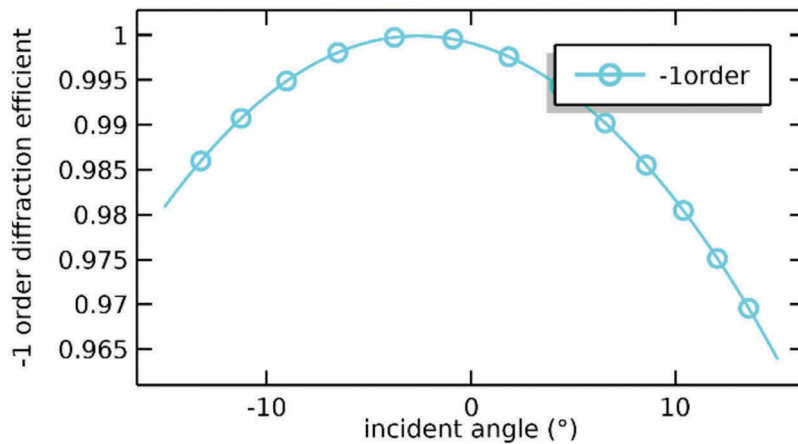


Figure 9. (Colour online) The simulation result of the incident angle response of PG diffraction efficiency, circular polarisation light for input. the grating period is 4 μm .

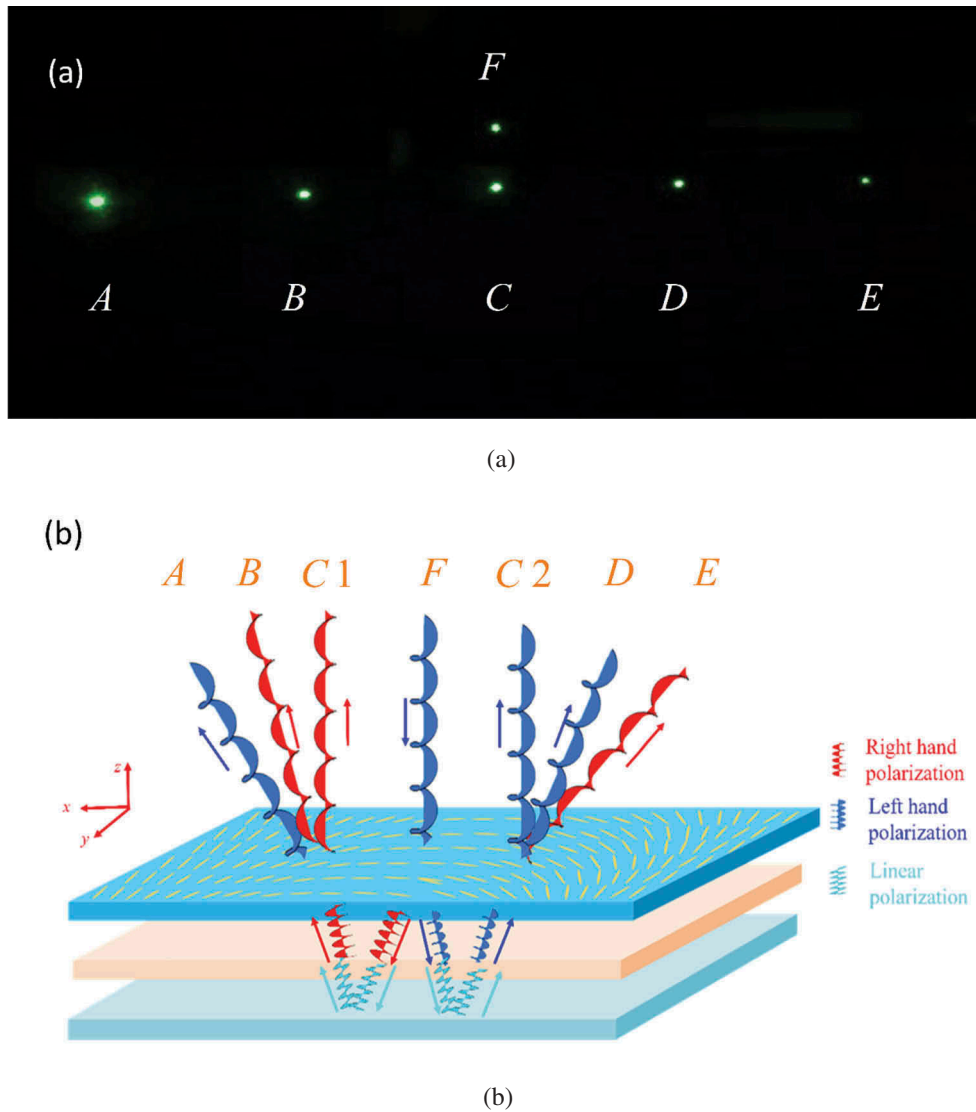


Figure 10. (Colour online) (a) The far-field diffraction of the reflective composite polarisation grating for left-handed circularly polarisation light, the grating period is 4 μm . (b) The schematic of optical performance when input light is along the negative z -axis into RCPG.

on the voltage applied to the cell which changes the polarisation state of beam before passed through the polarisation grating secondly. When the phase retardation of cell meets the quarter-wave condition, the power of light spot A is maximum, and it is 50 μW , the power of light spot B, light spot C, light spot D are about 14 μW which the light spot C dominate the power. The diffraction efficiency of spot A is over 75% which is lower than the simulation result 90%. The diffraction efficiency of the light spot A and B depends on the phase retardation of the PG and the diffraction efficiency of the light spot A and C depends on the polarisation state of beam before the beam hits into polarisation grating which is controlled by the quarter-wave plate and the mirror. The diffraction light beam goes through the quarter-wave plate twice

with different incident angles, so the polarisation state of the light beam before secondly incident into the polarisation grating is not perfect circular polarisation state. Thus, the diffraction efficiency of light spot A cannot be as high as the transmission mode of polarisation grating. The details of the quarter-wave plate and mirror need to be further optimised in order to improve the diffraction efficiency of RCPG.

6. Conclusion

In this article, we design a novel structure of polarisation grating called RCPG which can be fabricated simply and easily enlarge the deflection angle of polarisation grating. The deflection angle of RCPG is two times as large as the

transmission mode with the same grating period, which can be compared with polarisation volume grating or bragg polarisation grating. The theoretical diffraction efficiency of the RCPG can reach up to 90%, and the experimental diffraction efficiency is over 75% which could be further improved. Therefore, the RCPG with the large deflection angle and the high deflection efficiency could be a promising element in augmented reality system, polarimetry, beam steering and so on.

Acknowledgments

The authors are indebted to Rolic Company for their kind support with the photo-alignment material.

Disclosure statement

No potential conflict of interest was reported by the authors.

Funding

This work was supported by the The National Science Foundation of China [11604327, 11704377 and 61475152].

References

- [1] Chen HW, Lee JH, Lin BY, et al. Liquid crystal display and organic light-emitting diode display: present status and future perspectives. *Light Sci Appl*. 2018;7:17168.
- [2] Zhang Z, You Z, Chu D. Fundamentals of phase-only liquid crystal on silicon (LCOS) devices. *Light Sci Appl*. 2014;3:e213.
- [3] Avci N, Hwang SJ. Electrically tunable polarization independent blue-phase liquid crystal binary phase grating via phase-separated composite films. *Liq Cryst*. 2017;44:1–7.
- [4] Li H, Wang C, Pan Y, et al. Transient holographic grating in azo-dye-doped liquid crystals with off resonant light. *Liq Cryst*. 2016;44:1–6.
- [5] Chien CY, Sheu CR. Small dosage of holographic exposure via a He-Ne laser to fabricate tunable liquid crystal phase gratings operated with low electric voltages. *Liq Cryst*. 2016;44:1–9.
- [6] Chen P, Lu YQ, Hu W. Beam shaping via photo patterned liquid crystals. *Liq Cryst*. 2016;43:2051–2061.
- [7] Komanduri RK, Escuti MJ. Elastic continuum analysis of the liquid crystal polarization grating. *Phys Rev E*. 2007;76(2 Pt 1):021701.
- [8] Oh C, Escuti MJ. Numerical analysis of polarization gratings using the finite-difference time-domain method. *Phys Rev A*. 2007;76:4.
- [9] Oh C, Escuti MJ. Time-domain analysis of periodic anisotropic media at oblique media at oblique incidence: an efficient FDTD implementation. *Opt Exp*. 2006;14:11870.
- [10] Gao K, McGinty C, Payson H, et al. High efficiency large-angle Pancharatnam phase deflector based on dual-twist design. *Opt Exp*. 2017;25:6283.
- [11] Chen HH, Bhowmik AK, J.Bos P. Analysis of dual-twist Pancharatnam phase device with ultrahigh-efficiency large-angle optical beam steering. *Appl Opt*. 2015;54(34):10035–10043.
- [12] Chen HH, Bhowmik AK, J.Bos P. Concept for a transmissive, large angle, light steering device with high efficiency. *Opt Lett*. 2015;40(9):2080–2083.
- [13] Xiang X, Kim JW, Komanduri R. Nanoscale liquid crystal polymer Bragg polarization gratings. *Opt Express*. 2017;25(16):19298–19308.
- [14] Xiang X, Kim JW, Komanduri R. Bragg polarization gratings for wide angular bandwidth and high efficiency at steep deflection angles. *Sci Rep*. 2018;8:7202.
- [15] Lee YH, Yin K, Wu ST. Reflective polarization volume gratings for high efficiency waveguide-coupling augmented reality displays. *Opt Exp*. 2017;25(22):27008–27014.
- [16] Wei BY, Chen P, Ge SJ, et al. Fast-response and high efficiency optical switch based on dual-frequency liquid crystal polarization grating. *Opt Mater Exp*. 2016;6:597–602.
- [17] Lu YQ, Liang X, Wu YH, et al. Dual-frequency addressed hybrid-aligned nematic liquid crystal. *Appl Phys Lett*. 2004;85:3354–3356.
- [18] Li SZ, Liu YG, Liu CJ, et al. Electrically tunable photo-alignment hybrid double-frequency liquid crystal polarisation grating. *Liq Cryst*. 2018.
- [19] Tan L, Ho JY, Srivastava AK, et al. A simplified model for the optimization of LC photonic element. *IEEE Photonic Tech L*. 2014;26(11):1096–1099.
- [20] Tan L, Ho JY, Kwok HS. Extended Jones matrix method for oblique incidence study of polarization grating. *Appl Phys Lett*. 2012;101:051107.
- [21] Oh C, Escuti MJ. Achromatic diffraction from polarization gratings with high efficiency. *Opt Lett*. 2008;33(20):2287–2289.
- [22] Kim J, Oh C, Serati S, et al. Wide-angle, non-mechanical beam steering with high throughput utilizing polarization gratings. *Appl Opt*. 2011;50(17):2636–2639.
- [23] Weng YS, Xu DM, Zhang YN. Polarization volume grating with high efficiency and large diffraction angle. *Opt Exp*. 2016;24(16):17746–17759.
- [24] Li SZ, Zhao ZW, Wang CM, et al. Electrically tunable photo-aligned two-dimensional liquid crystal polarisation grating. *Liq Cryst*. 2018.
- [25] Chen H, Weng Y, Xu D, et al. Beam steering for virtual/augmented reality displays with a cycloidal diffractive wave plate. *Opt Exp*. 2016;24:7287.
- [26] Weng YS, Zhang YN, Cui JG, et al. liquid crystal based polarization volume grating applied for full color waveguide displays. *Opt Lett*. 2018;43(23):5773–5776.
- [27] Komanduri RK, Escuti MJ. High efficiency reflective liquid crystal polarization gratings. *Appl Phys Lett*. 2009;95:091106.
- [28] Crawford GP, Eakin JN, Radcliffe MD, et al. Liquid-crystal diffraction gratings using polarization holography alignment techniques. *J Appl Phys*. 2005;98(12):1671.
- [29] Wu H, Hu W, Hu H, et al. Arbitrary photo-patterning in liquid crystal alignments using DMD based lithography system. *Opt Exp*. 2012;20(20):16684–16689.